Computational Study of the Reactions of Methane with XO Radicals (X = F, Cl, or Br): Implications in Combustion Chemistry

Florent Louis,[†,§] Thomas C. Allison,[†] Carlos A. Gonzalez,[†,*] and Jean-Pierre Sawerysyn[‡]

Physical and Chemical Properties Division, National Institute of Standards and Technology, Gaithersburg, Maryland 20899-8381, USA, and Laboratoire de Cinétique et Chimie de la Combustion, UMR CNRS 8522, Centre d'Etudes et de Recherches Lasers et Applications (CERLA), Université des Sciences et Technologies de Lille, 59655 Villeneuve d'Ascq Cedex, France

Received: August 7, 2000; In Final Form: February 19, 2001

Theoretical calculations were carried out on the H atom abstraction reaction from methane by XO (X = F, Cl or Br) radical attack. Geometry optimizations and vibrational frequency calculations were performed using three methods: Møller−Plesset second-order perturbation theory (MP2), quadratic configuration interaction in the space of single and double excitations (QCISD), and the "hybrid" three-parameter exchange functional with Becke's gradient corrected exchange and Lee−Yang−Parr correlation functional (B3LYP). Single-point energy calculations were performed using several high quality basis sets. Canonical transition-state theory was used to predict the rate constants as a function of temperature (700−2500 K), and three-parameter Arrhenius expressions were obtained by fitting to the computed rate constants. The possible impact of the title reactions in combustion chemistry is also discussed.

Introduction

The theoretical treatment of combustion and thermal oxidation mechanisms can become time-consuming as the number of "heavy atoms" (non-hydrogen atoms) increases, especially if halogens such as Cl and Br are present. For many of these species, there is little or no information about the kinetics or mechanisms of the elementary reactions at elevated temperatures. Model development of thermal degradation processes of halogenated compounds in methane flames requires knowledge of kinetic and thermodynamic data characterizing the reactions between radicals of the type XO (X = F, Cl or Br) with methane. Until now, only an upper limit[1] and an estimation[2] of the Arrhenius expression of the rate constant for the reaction ClO + CH_4 have been reported in the literature. For the reaction BrO + CH_4, only an upper limit[3] to the rate constant has been reported. In addition, only one theoretical study related to the energetics of the FO + CH_4 reaction is available in the literature.[4] There are no theoretical rate constants calculations reported in the literature for the reactions of methane with ClO and BrO radicals.

In this work, the results of theoretical calculations are presented for the series of reactions

$$XO + CH_4 \rightarrow \text{products} \quad (X = F, Cl \text{ or } Br) \qquad (R1)$$

The following pathways for attack by XO radicals on methane are studied

$$\text{H atom abstraction } XO + CH_4 \rightarrow HOX + CH_3 \qquad (R1a)$$

$$\text{H/OX atom substitution } XO + CH_4 \rightarrow H + CH_3OX \qquad (R1b)$$

The main goal of this study is to assess the potential impact of pathways (R1a) and (R1b) in the thermal degradation of halogenated compounds as well as to provide rate constant expressions for these reactions so that they can be used in the modeling of combustion processes. This is particularly important in view of the lack of experimental data for these reactions.

Computational Methods[5]. All calculations were carried out with the Gaussian 94[6] suite of programs on a 4-processor Compaq PC and 32-processor Silicon Graphics Origin 2000 parallel computers. Throughout this paper, we adopt the following convention to indicate a particular computational procedure:

$Level_i/Basis_X$: indicates an optimization at the level of theory "i" using the basis set "X".

$Level_j/Basis_Y//Level_i/Basis_X$: indicates a single-point energy calculation at the level of theory "j" using the basis set "Y" on the geometry optimized at the level of theory "i" using the basis set "X".

In addition, the following levels of theory were used:

UMP2: Unrestricted second-order Møller−Plesset perturbation theory.[7]

PMP4(SDTQ): Fourth-order Møller−Plesset perturbation theory in the space of single, double, triple, and quadruple excitations with full annihilation of spin contaminant.[8]

QCISD: Quadratic configuration interaction level of theory in the space of single and double excitations.[9]

QCISD(T): Quadratic configuration interaction level of theory in the space of single and double excitations plus triple excitations treated perturbatively.[9]

B3LYP: Density functional theory (DFT) using the "hybrid" three-parameter exchange with Lee−Yang−Parr correlation functional (B3LYP).[10]

* To whom correspondence should be addressed. E-mail: (F. L.) florent.louis@univ-lille1.fr. Fax (33)-3-20436977, (C.G) carlos.gonzalez@nist.gov, Fax: (301)869-4020

† Physical and Chemical Properties Division, National Institute of Standards and Technology.

‡ Laboratoire de Cinétique et Chimie de la Combustion, UMR CNRS 8522, Centre d'Etudes et de Recherches Lasers et Applications (CERLA), Université des Sciences et Technologies de Lille.

§ Present address: See ‡.

10.1021/jp0028498 CCC: $20.00
Published on Web 04/05/2001

Geometric parameters of reactants, products and transition states were fully optimized at the UMP2/6-31G(d,p), QCISD/6-311G(d,p) and B3LYP/6-311G(d,p) levels. Harmonic vibrational frequencies were also calculated at these levels in order to characterize the nature of the stationary points on the potential energy surface and to compute zero-point energy corrections (used in the calculation of relative energies). Single-point energies were computed at the PMP4(SDTQ)/Basis//UMP2/6-31G(d,p), QCISD(T)/Basis//QCISD/6-311G(d,p), and B3LYP/Basis//B3LYP/6-311G(d,p) levels of theory, with "Basis" ranging from Pople-style sets[11] to the augmented correlation-consistent polarized valence triple-ζ sets (aug-cc-pVTZ) developed by Kendall et al.[12] and Wilson et al.[13] for the bromine atom. The reason for using these different approaches was to assess the accuracy of the results predicted by the Møller−Plesset perturbation theory and DFT relative to the highly correlated (and significantly more computationally demanding) QCISD and QCISD(T) results. This is particularly relevant in the case of B3LYP, which formally scales as $O(N^3)$, in contrast to MP2 which scales as $O(N^5)$ and QCISD which scales as $O(N^6)$, where N is the number of basis set functions used.

Canonical transition state theory[14] (TST) including semiclassical multiplicative tunneling correction factors was used to predict the temperature dependence of the rate constants. The rate constants, $k(T)$, were computed using the following expression

$$k(T) = \Gamma(T) \times \frac{k_B T}{h} \times \frac{Q_{TS}(T)}{Q_{XO}(T) Q_{CH_4}(T)} \times \exp\left(-\frac{V_a^G}{k_B T}\right) \quad (1)$$

where $\Gamma(T)$ indicates the transmission coefficient used for the tunneling correction at temperature T, $Q_{TS}(T)$, $Q_{XO}(T)$, and $Q_{CH4}(T)$ are the total partition functions for the transition state (TS), XO radical, and methane at temperature T; V_a^G is the vibrationally adiabatic barrier height computed as the difference in energies between transition states and reactants and including zero point energy corrections, k_B is Boltzman's constant, and h is Planck's constant. The calculation of the reaction rate constants using the TST formulation given by eq 1 requires the proper computation of the partition functions of reactants and the transition states. The total partition function $Q_X(T)$ of species X (X = CH_4, XO, or TS) can be cast in terms of the translational (Q_T), rotational (Q_R), electronic (Q_e), and vibrational (Q_v) partition functions. The multiplicity of the $^2\Pi_{3/2}$ and $^2\Pi_{1/2}$ states as well as the energy gaps of 193.8 cm^{-1} for FO, 320.3 cm^{-1} for ClO, and 968 cm^{-1} for BrO between the low-lying electronic states[15] have been explicitly included in the computation of the electronic partition function for the XO radicals.

Vibrations were treated as harmonic oscillators with the exception of the $H_3C\cdot\cdot H\cdot\cdot OX$ (X = F, Cl, or Br) torsional mode of the transition state. This mode was treated as a hindered internal rotor and removed from the vibrational partition function for the TS. The corresponding hindered rotor partition function, $Q_{HR}(T)$, was calculated by the method devised by Ayala and Schlegel,[16] and it was further included in the expression for the rate constant as explained in our previous study dealing with the reactions of OH radicals with dibromomethane (CH_2Br_2).[17]

We adopt the simple and computationally inexpensive Wigner method[18] in the calculation of all tunneling corrections for the reactions reported in this work

$$\Gamma(T) = 1 + \frac{1}{24}\left(\frac{h\nu^{\ddagger}}{k_B T}\right)^2 \quad (2)$$

TABLE 1: Reaction Enthalpies at 298 K and $k_{(H\ atom\ abstraction)}/k_{(H/-OX\ substitution)}$ = F(T) Calculated at the PMP2/6-31G(d,p)//MP2/6-31G(d,p) Level for the Series of Reactions XO + CH_4 → Products at Three Temperatures

		$k_{(H\ atom\ abstraction)}/k_{(H/-OX\ substitution)}$[b]		
	$\Delta_r H^a$ (298 K)	700 K	1500 K	2500 K
FO + CH_4	19.7 (63.9)[c]	3.3×10^{11}	2.1×10^5	1.1×10^3
ClO + CH_4	19.4 (77.1)	1.3×10^{12}	3.3×10^5	1.3×10^3
BrO + CH_4	5.5 (67.4)	8.4×10^{11}	2.6×10^5	1.1×10^3

[a] Including the sum of thermal energies = ΔZPE + thermal energy corrections. [b] Rate constants for both pathways are calculated using Wigner's correction. [c] The values in parentheses correspond to the values obtained for the substitution reactions.

where $\nu^{\ddagger}$ is the imaginary frequency at the saddle point. This choice seems to be appropriate to the tunneling corrections applied to the rate constants calculated at typical incineration/combustion temperatures (700−2500 K) for which the values of transmission coefficient $\Gamma(T)$ are generally small or moderate (≤ 2).[19] Rate constant calculations were carried out over the temperature range of interest using the Turbo-Opt program.[20]

Results and Discussion

To assess the relative importance of the substitution pathway compared to the abstraction channel, calculations (full geometry optimization and vibrational frequencies) were carried out for both pathways at the UMP2/6-31G(d,p) level. In addition, reaction enthalpies at 298 K and the ratios $k_{(H\ atom\ abstraction)}/k_{(H/-OX\ substitution)}$ at 700, 1500, and 2500 K were computed at the PMP2/6-31G(d,p)//UMP2/6-31G(d,p) level. The results of these calculations (Table 1) show that the H/-OX substitution pathway cannot compete with the H atom abstraction pathway in the temperature range considered in this study (700−2500 K). Consequently, it is concluded that the series of reactions of methane with XO radicals are more likely to proceed via pathway (R1a) instead of (R1b). Detailed results for pathway (R1a) are presented and discussed in the remainder of this paper.

1. Geometric Parameters and Vibrational Frequencies. *Geometric parameters.* Table 2 lists the essential structural parameters calculated for the three transition states. More detailed information regarding optimized geometric parameters, vibrational frequencies and unscaled zero-point energy corrections for reactants, products, and transition state structures are presented in the Tables 1S-6S of the Supporting Information.

As observed in Table 2, regardless of the level of theory, the abstraction reactions of the XO radicals with methane are characterized by transition structures with a nearly linear C−H−O angle. UMP2 predicts a relatively "early" transition state on the potential energy surface, where the breaking C−H bond is stretched by only a small amount from its equilibrium value of 1.086 Å in CH_4. On the other hand, the forming O−H bond is still relatively long, compared to the equilibrium values in HOX (0.971−0.972 Å as reported in the Supporting Information section). In addition, we notice that UMP2 predicts shorter C−H bonds and longer O−H bonds when compared to the corresponding QCISD and B3LYP values.

Vibrational Frequencies. The values of the imaginary frequency, calculated by ab initio methods for each transition state, suggest that tunneling through the barrier may be important at atmospheric temperatures. The B3LYP imaginary frequencies (expressed in cm^{-1}) of 1570*i* (FO), 1575*i* (ClO), and 1577*i* (BrO) are found to be considerably lower than those calculated by MP2 or QCISD (Table 2). In all cases, the reaction coordinate is characterized by migration of the hydrogen being abstracted

TABLE 2: Essential Structural Parameters[a], Imaginary Vibrational Frequencies for the Transition State of Each Reaction, and Internal Rotation Barrier of the −OX Group at Different Levels of Theory[b]

		r (C−H_R)	r (O−H_R)	(θOH_RC)	(ϕXOH_RC)	$\nu^{\neq}$ cm^{-1}	V_0, kJ mol^{-1}
FO + CH_4	1)	1.235	1.243	176.7	0.0	2169i	0.55
	2)	1.289	1.209	180.0	0.0	2285i	0.45
	3)	1.346	1.175	179.8	0.0	1570i	0.50
ClO +CH_4	1)	1.231	1.251	177.0	0.1	2073i	0.45
	2)	1.291	1.203	177.9	−0.1	2298i	0.55
	3)	1.353	1.166	179.2	−41.1	1575i	0.40
BrO +CH_4	1)	1.217	1.273	176.0	48.8	2152i	0.65
	2)	1.286	1.207	178.1	52.0	2280i	0.65
	3)	1.346	1.169	179.4	77.8	1577i	0.50

[a] Bond lengths are in angstroms, bond angles θ are in degrees; the hydrogen atom involved in H atom abstraction is noted H_R [b] The different levels of theory used in this study for the geometry optimization are the following: 1) UMP2/6-31G(d,p), 2) QCISD/6-311G(d,p), 3) B3LYP/6-311G(d,p)

TABLE 3: Reaction Enthalpies Δ_rH at 298 K and Barrier Heights V_a^G Calculated in kJ Mol^{-1} for the Reaction FO + CH_4 → HOF + CH_3 at Various Levels of Theory

	$\Delta_r H$[a]			V_a^G		
basis sets	**PMP4**[b]	**QCISD(T)**[c]	**B3LYP**[d]	**PMP4**[b]	**QCISD(T)**[c]	**B3LYP**[d]
6-311G(d,p)	25.9	35.6	39.3	62.8	70.4	43.3
6-311+G(d,p)	18.0	28.5	30.5	60.1	66.3	41.4
6-311++G(d,p)	17.6	28.0	30.1	59.6	65.7	41.1
6-311++G(2d,p)	19.2	31.0	30.1	60.1	66.1	42.0
6-311++G(2d,2p)	13.8	25.1	28.0	59.5	65.3	42.0
6-311++G(2df,2p)	15.5	37.7	30.1	57.4	63.7	43.3
6-311++G(3df,2p)	15.1	25.9	29.3	56.6	62.9	42.8
6-311++G(3df,2pd)	12.1	23.0	28.5	53.2	59.5	42.1
6-311++G(3df,3pd)	10.5	21.3	27.6	49.5	55.7	40.7
aug-cc-pVTZ	12.1	24.3	33.1	52.2	58.3	46.9
literature[e]		14.2 ± 15.6				

[a] Including the sum of thermal energies = ΔZPE + thermal energy corrections. [b] Optimized geometries at the UMP2/6-31G(d,p) level of theory. [c] Optimized geometries at the UQCISD/6-311G(d,p) level of theory. [d] Optimized geometries at the B3LYP/6-311G(d,p) level of theory. [e] based on the formation enthalpies taken for FO, CH_4, HOF, and CH_3 from the literature (see supplementary Table 7S of the Supporting Information).

TABLE 4: Reaction Enthalpies $\Delta_r H$ at 298 K and Barrier Heights V_a^G Calculated in kJ mol^{-1} for the Reaction ClO + CH_4 → HOCl + CH_3 at Various Levels of Theory

	$\Delta_r H$[a]			V_a^G		
basis sets	**PMP4**[b]	**QCISD(T)**[c]	**B3LYP**[d]	**PMP4**[b]	**QCISD(T)**[c]	**B3LYP**[d]
6-311G(d,p)	23.0	34.3	43.9	51.8	67.3	48.2
6-311+G(d,p)	19.2	32.2	42.3	51.6	67.3	52.2
6-311++G(d,p)	18.8	32.2	42.3	50.7	66.7	52.0
6-311++G(2d,p)	26.8	40.6	46.9	56.0	72.2	57.2
6-311++G(2d,2p)	20.5	33.9	44.8	55.2	71.0	57.0
6-311++G(2df,2p)	24.3	48.1	48.5	55.4	71.1	59.9
6-311++G(3df,2p)	26.4	39.3	49.4	55.6	71.7	60.5
6-311++G(3df,2pd)	23.4	36.0	49.0	52.2	68.1	59.8
6-311++G(3df,3pd)	21.8	34.3	48.1	48.8	64.5	58.5
aug-cc-pVTZ	21.8	35.1	51.9	49.4	65.5	64.2
literature[e]		45.4 ± 3.6				

[a] Including the sum of thermal energies = ΔZPE + thermal energy corrections. [b] Optimized geometries at the UMP2/6-31G(d,p) level of theory. [c] Optimized geometries at the UQCISD/6-311G(d,p) level of theory. [d] Optimized geometries at the B3LYP/6-311G(d,p) level of theory. [e] based on the formation enthalpies taken for ClO, CH_4, HOCl and CH_3 from the literature (see supplementary Table 7S of the Supporting Information).

from the carbon atom toward the oxygen. For each transition state, low frequencies (about 30−40 cm^{-1}) corresponding to the $H_3C\cdot\cdot H\cdot\cdot OX$ (X = F, Cl, or Br) torsional mode were found and treated as a hindered rotor as explained in the Computational Methods section.

To compute the hindered rotor partition function corresponding to the transition states, $Q_{HR}(T)$, the height of the energy barrier to rotation, V_0, and the periodicity, σ, of the torsion potential must be estimated. These parameters were obtained by performing a rigid scan in the CHOX dihedral where this angle was varied from 0° to 360° using a 15° interval. For the three reactions of interest, the torsion potentials were found to be 3-fold (σ = 3), with an internal rotation barrier V_0 of about 0.5 kJ mol^{-1} (Table 2). Given the relatively small rotational barriers, in reality these modes behave as free-rotors in the temperature range 700−2500 K.

2. Reaction Enthalpies at 298 K and Barrier Heights. Tables 3−5 list the reaction enthalpies ($\Delta_r H$) and barrier heights computed at different levels of theory for all H atom abstraction reactions under study.

Reaction Enthalpies at 298 K. To determine whether the levels of theory used in this study are appropriate, reaction enthalpies at 298 K have been computed for the three H atom abstraction reactions and the results compared to the available experimental data. The computed $\Delta_r H$ values are listed in Tables 3−5, whereas the literature values of the formation enthalpies, $\Delta_f H°$ at 298 K, for the species of interest are provided in the Supporting Information (Table 7S).

TABLE 5: Reaction Enthalpies $\Delta_r H$ at 298 K and Barrier Heights V_a^G Calculated in kJ Mol^{-1} for the Reaction BrO + CH_4 → HOBr + CH_3 at Various Levels of Theory

	$\Delta_r H^a$			Va^G		
basis sets	**PMP4**[b]	**QCISD(T)**[c]	**B3LYP**[d]	**PMP4**[b]	**QCISD(T)**[c]	**B3LYP**[d]
6-311G(d,p)	11.7	26.6	38.5	45.5	62.2	46.2
6-311+G(d,p)	6.2	23.8	35.2	43.9	61.2	48.3
6-311++G(d,p)	5.9	23.5	35.2	43.3	60.5	48.2
6-311++G(2d,p)	14.1	32.1	37.7	47.1	65.1	51.1
6-311++G(2d,2p)	7.6	25.4	35.6	46.2	63.8	51.3
6-311++G(2df,2p)	10.6	39.0	38.9	45.8	63.6	54.0
6-311++G(3df,2p)	11.4	28.5	38.5	46.1	64.0	53.9
6-311++G(3df,2pd)	8.0	25.2	37.7	42.8	60.4	53.1
6-311++G(3df,3pd)	6.6	23.8	37.2	39.7	57.0	52.1
aug-cc-pVTZ	10.0	27.3	41.5	38.9	57.1	55.2
literature[e]		38.9 ± 11.3				

[a] Including the sum of thermal energies = ΔZPE + thermal energy corrections. [b] Optimized geometries at the UMP2/6-31G(d,p) level of theory. [c] Optimized geometries at the UQCISD/6-311G(d,p) level of theory. [d] Optimized geometries at the B3LYP/6-311G(d,p) level of theory. [e] On the basis of the formation enthalpies taken for BrO, CH_4, HOBr, and CH_3 from the literature (see supplementary Table 7S of the Supporting Information).

The results in Tables 3−5 indicate that adding one diffuse function on the heavy atoms to the basis sets leads to a decrease in the reaction enthalpy values of up to 8 kJ mol^{-1} for the FO + CH_4 reaction. This effect is slightly smaller in the case of ClO and BrO (−2 to −5 kJ mol^{-1}). Furthermore, adding a diffuse function on the hydrogen atoms does not seem to change significantly the reaction enthalpies ($\Delta\Delta_r H$ < −0.5 kJ mol^{-1}). No significant trend is observed after adding extra p-, d-, and f-polarization functions. However, in all three cases, the results obtained with the relatively large 6-311++G(3df,3pd) basis set seem to agree reasonably well with the aug-cc-pVTZ values.

Overall, the reaction enthalpies for the FO + CH_4 reaction calculated at the PMP4(SDTQ) level with basis sets that have diffuse functions are very close to the literature values, whereas QCISD(T) and B3LYP on the other hand, overestimate the experimental value by about 7 to 25 kJ mol^{-1}. The opposite trend is observed in the case of the reactions involving ClO and BrO. This behavior can be attributed to errors arising from truncation in the basis sets as well as insufficient treatment of correlation effects, which lead to erratic trends resulting from an unbalance in the treatment of the electronic structure problem of the different species involved in the reactions. Direct comparison with the experimental data, however, must be considered with care in view of the large experimental uncertainties reported, especially in the case of the reaction FO + CH_4 → FOH + CH_3, where the uncertainty is larger than the actual value (see Table 3).

Barrier Heights. In the case of the FO + CH_4 reaction (Table 3), the V_a^G's calculated with the B3LYP density functional are systematically lower by 5 to 30 kJ mol^{-1} when compared to those obtained with the correlated ab initio methods PMP4 (SDTQ) and QCISD(T) (which are in good agreement with those reported previously by Francisco[4]). For the ClO and BrO reactions, the B3LYP barriers are in better agreement with the PMP4(SDTQ) values when relatively small basis sets are used. However, in the case of larger basis sets (especially aug-cc-pVTZ), B3LYP seems to predict V_a^G's in better agreement with the results obtained by the highly correlated method QCISD(T). In this work, we choose the aug-cc-pVTZ basis set in order to compute the energetics and reaction rate constants as explained in the Computational Methods section.

3. Rate Constants Calculations. The three-parameter Arrhenius expressions $k(T) = B \times T^n \exp(-E_a/RT)$ fitted to the computed rate constants are listed in Table 6. A list of calculated rate constants with the aug-cc-pVTZ basis set (FO, ClO, and BrO reactions) is provided in the Supporting Information (Table 8S).

TABLE 6: Summary of the Arrhenius Parameters $K = B \times T^n \exp(-E_a/RT)$ Calculated over the Temperature Range 700−2500 K Using the aug-cc-pVTZ Basis Set

		B, cm^3 molecule^{-1} s^{-1}	n	E_a/R, K
FO +CH_4	**PMP4(SDTQ)**	1.9×10^{-20}	2.65	4920
	QCISD(T)	5.0×10^{-21}	2.84	5375
	B3LYP	6.0×10^{-21}	2.83	4495
ClO +CH_4	**PMP4(SDTQ)**	3.8×10^{-21}	2.84	4470
	QCISD(T)	3.0×10^{-21}	2.89	6365
	B3LYP	7.9×10^{-21}	2.79	6645
BrO +CH_4	**PMP4(SDTQ)**	1.4×10^{-20}	2.68	3320
	QCISD(T)	1.3×10^{-20}	2.71	5530
	B3LYP	1.7×10^{-20}	2.71	5620

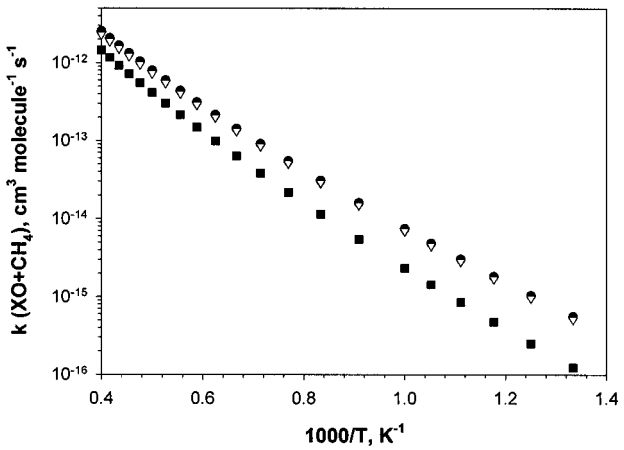

Figure 1. Rate constants vs 1/T over the temperature range 700−2500 K for the H atom abstraction reactions of CH_4 with FO (filled circles), ClO (filled squares), and BrO (open triangles) at the QCISD-(T) level of theory.

Figure 1 shows a marked curvature of the Arrhenius plots over the temperature range (700−2500 K).[21] In addition, it is observed that over the same temperature range, the rate constants for the reaction FO + CH_4 are very close to the corresponding values of the reaction BrO + CH_4. In turn, these two reactions exhibit rate constants approximately two times larger than the rate constants for ClO + CH_4. This is in keeping with the fact that the barriers for these two reactions are smaller than the corresponding barrier for ClO + CH_4. On the basis of the relative electronegativity of F, Cl, and Br, one would expect the barriers for the series of reactions CH_4 + XO to follow the trend FO < ClO < BrO. However, as discussed before, our results show a very different trend, with FO ≈ BrO < ClO. This trend might be explained in terms of the "π-donor" and

"σ-acceptor" capabilities of the halogen atoms and their effects on the relative bond strength of the H−OX bond. Thus, the relatively high "σ-acceptor" character of fluorine stabilizes the H−OX bond considerably. In the case of chlorine, this stabilization is somehow reduced by the interaction between one of the lone pairs (with p-character) and the lone-pair electron located in the oxygen atom, as a result of its relatively large "π-donor" character. Finally, given that the "π-donor" character in bromine is significantly smaller when compared to chlorine, these repulsions are smaller and consequently the H−OBr bond becomes stronger than the corresponding H−OCl bond.

The values of 5.1×10^{-16} cm^3 molecule^{-1} s^{-1}, 3.3×10^{-17} cm^3 molecule^{-1} s^{-1}, and 3.0×10^{-17} cm^3 molecule^{-1} s^{-1} calculated at 670 K, respectively, with PMP4(SDTQ), QCISD (T), and B3LYP for the rate constant of the ClO + CH_4 reaction are well below the upper limit value of 4.0×10^{-15} cm^3 molecule^{-1} s^{-1} proposed by Clyne and Watson.[1] It is noteworthy that the rate constant values for the ClO + CH_4 reaction calculated in the temperature range 700−2000 K using the three theoretical methods (Table 6) are larger than the values obtained from the Arrhenius expression $k = 1.7 \times 10^{-9} \exp(-15\,500/T)$ in cm^3 molecule^{-1} s^{-1} (or $1.0 \times 10^{12} \exp(-15\,500/T)$ in L mol^{-1} s^{-1}) estimated by Baulch et al.[2] In addition, in the temperature range 2000−2500 K, all values are in good agreement. To the best of our knowledge, no experimental concentration profiles of the ClO radical have been reported in the laboratory studies devoted to the thermal treatment of chlorinated methanes in methane flames. Bouhria[22] has compared the rates of production and consumption of HOCl calculated from a chemical model proposed for a $CH_4/O_2/Ar$ + 2.2% CH_3Cl flat flame. On the basis of the estimated Arrhenius expression proposed by Baulch et al.,[2] he suggested that the ClO + CH_4 reaction was the main reaction responsible for the production of HOCl close to the surface of the flat flame burner. The lack of experimental data on the ClO concentrations does not enable us to compare the rate of ClO + CH_4 reaction with the ones of reactions Cl + CH_4 and OH + CH_4, which play an important role in the consumption of methane. However, from our calculations showing relatively low rate constants ($k \approx 10^{-15}-10^{-14}$ cm^3 molecule^{-1} s^{-1} at 1000 K and $k \approx 2 \times 10^{-12}$ cm^3 molecule^{-1} s^{-1} at 2500 K) for ClO + CH_4 reactions, it would seem that the H atom abstraction reactions of ClO radicals with CH_4 cannot compete with OH + CH_4 ($k \approx 1.4 \times 10^{-12}$ cm^3 molecule^{-1} s^{-1} at 1000 K[23]) and Cl + CH_4 ($k \approx 8.2 \times 10^{-12}$ cm^3 molecule^{-1} s^{-1} at 1000 K[23]) to consume CH_4 in the thermal degradation processes of chlorinated compounds in methane flames.

In the case of the reaction of BrO with methane, only one upper limit at 293 K was reported by Clyne and Cruse[3] ($<1.7 \times 10^{-14}$ cm^3 molecule^{-1} s^{-1}). This value cannot be compared with the values calculated in this study for a temperature range 700−2500 K.

Even though the Arrhenius parameters obtained with B3LYP are in better agreement with the corresponding values computed at the QCISD(T) level in the case of ClO and BrO when compared to the PMP4(SDTQ) results, the opposite trend is observed in the case of FO. Given the lack of a definitive trend in the accuracy of the less computationally intensive methodologies B3LYP and PMP4(SDTQ), we recommend the Arrhenius parameters computed with our best theoretical level, QCISD (T), for use in the modeling of combustion processes involving the abstraction reactions discussed in this work. However, care must be exercised when using these parameters, given the lack of experimental data needed for the appropriate validation of the methodology used in their computation. We believe that the use of these parameters might at least provide a semiquantitative picture of the kinetics of these reactions, especially at temperatures typical of incineration/combustion processes. This lack of reactivity, however, does not preclude the XO radicals from participating in other reactions of combustion significance.

Conclusions

Ab initio electronic structure calculations, combined with canonical Transition State Theory, carried out on the H/−OX substitution reactions XO + $CH_4 \rightarrow$ H + CH_3OX (X = F, Cl, or Br), lead to the conclusion that the substitution pathways are not competitive with the abstraction pathways over the temperature range under study (700−2500 K) given that these processes are characterized by lower rate constants than those obtained for the H atom abstraction reactions XO + $CH_4 \rightarrow$ HOX + CH_3. In addition, it is found that all levels of theory used in this work calculations predict relatively low rate constants for the H atom abstraction reactions in the studied temperature range, suggesting that these pathways might not be important in the degradation processes of halogenated compounds.

Acknowledgment. The authors thank the CERLA for providing computing time for part of the theoretical calculations under project MUST. We are also grateful to the ≪Ministère de la Recherche et de l'Enseignement Supérieur≫, the ≪Région Nord/Pas de Calais≫, and the ≪Fonds Européen de Développement Economique des Régions≫ (FEDER) for partial funding of this work and for supporting CERLA. The authors also thank Dr. Robert E. Huie and Dr. Michael J. Kurylo for helpful discussions.

Supporting Information Available: Tables of (i) the optimized geometry parameters of the reactants, products, and transition states (supplementary Tables 1S-4S), (ii) their vibrational frequencies (supplementary Tables 5S-6S), (iii) the values of the literature heats of formation (supplementary Table 7S), and (iv) the values of the computed rate constants as a function of temperature (supplementary Table 8S). This material is available free of charge via the Internet at http://pubs.acs.org.

References and Notes

(1) Clyne, M. A. A.; Watson, R. T. *J. Chem. Soc., Faraday Trans. 1* **1974**, *70*, 2250.

(2) Baulch, D. L.; Duxbury, J.; Grant, S. J.; Montague, D. C. *J. Phys. Chem. Ref. Data*, **1981**, Supl. 1, 10.

(3) Clyne, M. A. A.; Cruse, H. W. *J. Chem. Soc. Faraday. Trans.* **1970**, *66*, 2227.

(4) Francisco, J. S.; Su, Y. *Chem. Phys. Lett.* **1993**, *215*, 417.

(5) The identification of commercial equipment or materials does not imply recognition or endorsement by the National Institute of Standards and Technology, nor does it imply that the material or equipment identified are necessarily the best available for the purpose.

(6) Frisch, M. J.; Trucks, G. W.; Schlegel, H. B.; Gill, P. M. W.; Johnson, B. G.; Robb, M. A.; Cheeseman, J. R.; Keith, T.; Petersson, G. A.; Montgomery, J. A.; Raghavachari, K.; Al-Laham, M. A.; Zakrzewski, V. G.; Ortiz, J. V.; Foresman, J. B.; Cioslowski, J.; Stefanov, B. B.; Nanayakkara, A.; M. Challacombe; Peng, C. Y.; Ayala, P. Y.; Chen, W.; Wong, M. W.; Andres, J. L.; Replogle, E. S.; Gomperts, R.; Martin, R. L.; Fox, D. J.; Binkley, J. S.; Defrees, D. J.; Baker, J.; Stewart, J. P.; Head-Gordon, M.; Gonzalez, C.; Pople, J. A. *GAUSSIAN 94*; Revision D.4 Gaussian, Inc: Pittsburgh, PA, 1995.

(7) Møller, C.; Plesset, M. S. *Phys. Rev.* **1934**, *46*, 618.

(8) (a) Schlegel, H. B. *J. Chem. Phys.* **1986**, *84*, 4530. (b) Schlegel, H. B. *J. Phys. Chem.* **1988**, *92*, 3075. (c) Sosa, C.; Schlegel, H. B. *Int. J. Quantum Chem.* **1986**, *29*, 1001. (d) Sosa, C.; Schlegel, H. B. *Int. J. Quantum Chem.* **1987**, *30*, 155.

(9) Pople, J. A.; Head-Gordon, M.; Raghavachari, K. *J. Chem. Phys.* **1987**, *87*, 5968.

(10) Becke, A. D. *J. Chem. Phys.* **1993**, *98*, 5648.

(11) Descriptions of the Pople-style basis sets can be found in the following: Foresman, J. B.; Frisch, A. E. *Exploring Chemistry with Electronic Structure Methods*, 2nd Ed.; Gaussian, Inc.: Pittsburgh, PA, 1996.

(12) Kendall, R. A.; Dunning, Jr. T. H.; Harrison, R. J. *J. Chem. Phys.* **1992**, *96*, 6796.

(13) Wilson, A. K.; Woon, D. E.; Peterson, K. A.; Dunning, T. H., Jr. *J. Chem. Phys.* **1999**, *110*, 7667.

(14) (a) Johnston, H. S. *Gas-Phase Reaction Rate Theory*; The Roland Press Company: New York, 1966. (b) Laidler, K. J. *Theories of Chemical Reaction Rates*; McGraw-Hill: New York, 1969. (c) Weston, R. E.; Schwartz, H. A. *Chemical Kinetics*; Prentice Hall: New York, 1972. (d) Rapp, D. *Statistical Mechanics*; Holt, Reinhard, and Winston: New York, 1972. (e) Nikitin, E. E. *Theory of Elementary Atomic and Molecular Processes in Gases*; Claredon Press: Oxford, 1974. (f) Smith, I. W. M. *Kinetics and Dynamics of Elementary Gas Reactions*; Butterworth: London, 1980. (g) Steinfeld, J. I.; Francisco, J. S.; Hase, W. L. *Chemical Kinetics and Dynamics*; Prentice Hall: New Jersey, 1989.

(15) NIST-JANAF, Thermochemical Tables, Fourth Edition, *J. Phys. Chem. Ref. Data*, 1998, Monograph N°9, Malcolm W. Chase Jr.

(16) Ayala, P. Y.; Schlegel, H. B. *J. Chem. Phys.* **1998**, *108*, 2314.

(17) Louis, F.; Gonzalez, C. A.; Huie, R. E.; Kurylo, M. J. *J. Phys. Chem. A*, **2000**, *104*, 2931.

(18) Wigner, E. P. *Z. Phys. Chem.* **1932**, *B19*, 203.

(19) Bell, R. P. *The Tunnel Effect in Chemistry*; Chapman and Hall: New York, 1980.

(20) Rate constants calculated with the Turbo-Rate module in the beta version of the TURBO−OPT geometry optimization package, developed by C. Gonzalez and T. Allison, National Institute of Standards and Technology, Gaithersburg, MD.

(21) The same trends were observed in the case of the Arrhenius plots predicted by B3LYP and PMP4(SDTQ) methods.

(22) Bouhria, M. Thesis of the University of Orléans, France, 1994.

(23) NIST Standard Reference Database 17−2Q98, National Institute of Standards and Technology, Gaithersburg, MD, 20899.